COMMUNICATIONS CHEMISTRY

ARTICLE

https://doi.org/10.1038/s42004-019-0187-3 OPEN

Nucleophilic reactivity of a copper(II)-hydroperoxo complex

Bohee Kim[1], Donghyun Jeong[1], Takehiro Ohta[2,3] & Jaeheung Cho[1]

Copper(II)-hydroperoxo species are often detected as key intermediates in metalloenzymes and biomimetic compounds containing copper. However, the only reactivity has previously been observed for the copper(II)-hydroperoxo complexes is electrophilic, occurring through O-O bond cleavage. Here we report that a mononuclear end-on copper(II)-hydroperoxo complex, which has been successfully characterized by various physicochemical methods including UV-vis, rRaman, CSI-MS and EPR, is a reactive oxidant that utilizes a nucleophilic mechanism. In addition, DFT calculations fully support the electronic structure of this complex as a copper(II)-hydroperoxo complex with trigonal bipyramidal coordination geometry. A positive Hammett ρ value (2.0(3)) is observed in the reaction of copper(II)-hydroperoxo complex with *para*-substituted acyl chlorides, which clearly indicates nucleophilic character for the copper(II)-hydroperoxo complex. The copper(II)-hydroperoxo complex is an especially reactive oxidant in aldehyde deformylation with 2-PPA and CCA relative to the other metal-bound reactive oxygen species reported so far. The observation of nucleophilic reactivity for a copper(II)-hydroperoxo species expands the known chemistry of metal-reactive oxygen species.

[1] Department of Emerging Materials Science, DGIST, 42988 Daegu, Korea. [2] Picobiology Institute, Graduate School of Life Science, University of Hyogo, RSC-LP Center, 679-5148 Hyogo, Japan. [3] Present address: Faculty of Engineering, Department of Applied Chemistry, Sanyo-Onoda City University, 756-0884 Sanyo-Onoda, Yamaguchi, Japan. Correspondence and requests for materials should be addressed to J.C. (email: jaeheung@dgist.ac.kr)

Copper-bound reactive oxygen adducts, such as Cu-superoxo, -peroxo, -hydroperoxo, and -oxyl radical species, have been proposed to be reactive intermediates in biological systems[1,2]. One such intermediate, specifically a Cu(II)-hydroperoxo complex, has received much attention since it has been hypothesized to play an important role in the catalytic cycle of certain copper-containing enzymes (Fig. 1). In peptidylglycine-α-hydroxylating monooxygenase (PHM) and dopamine-β-monooxygenase (DβM), it has been proposed that Cu(II)-hydroperoxo species were converted to Cu(II)-oxyl radicals and water after electron and proton transfers[3–5]. The reactive species in lytic polysaccharide monooxygenases (LPMOs) has also been proposed to be a Cu(II)-hydroperoxo intermediate that directly reacts with polysaccharides[6–9].

In synthetic chemistry, a number of Cu(II)-OOH species have been prepared and characterized by spectroscopic and crystallographic methods. Masuda's group reported the first crystal structure of the Cu(II)-OOH complex bearing a trigonal bipyramidal ligand where the hydroperoxo bound Cu(II) core was stabilized through intramolecular hydrogen bonding interactions[10]. Most recently, stabilization of $[Cu(biot\text{-}et\text{-}dpea)(OOH)]^+$ has been achieved in artificial proteins by using antigen-antibody interaction[11]. In general, the reaction of Cu(II)-OOH complexes with substrates occurs through O–O bond cleavage to give putative Cu(II)-oxyl radical or Cu(III)-oxo species. Detailed studies on the ligand hydroxylation by the putative intermediates have been reported by Karlin and co-workers[12]. Recently, it was also reported that the cleavage of Cu–O bond in Cu(II)-OOH species results in the *N*-dealkylation through the Fenton chemistry[13].

Notably, to our knowledge no reports of direct reactions of Cu(II)-OOH species with external substrates, i.e., prior to O–O bond cleavage, have yet appeared in the literature, although numerous examples of electrophilic reactivity in Cu(II)-OOH complexes have been shown to occur via O–O bond cleaved intermediates[14–16]. By contrast the nucleophilic reaction of Cu(II)-alkylperoxo complexes was reported very recently[17].

Herein, we report the nucleophilic reactivity of the Cu(II)-hydroperoxo complex, $[Cu(^{i}Pr_3\text{-tren})(OOH)]^+$ (**1**, $^{i}Pr_3$-tren = tris[2-(isopropylamino)ethyl]amine), which we find is capable of oxidation of organic carbonyl compounds directly. **1** was successfully characterized by various spectroscopic methods such as UV-vis, resonance Raman (rRaman), and electron paramagnetic resonance (EPR) spectroscopy together with cold spray ionization mass spectrometry (CSI-MS). The nucleophilic reactivity of **1** has also been investigated by kinetic studies including a Hammett analysis.

Results

Synthesis and characterization of copper complexes. As a starting material, the copper(II) complex, $[Cu(^{i}Pr_3\text{-tren})(CH_3CN)]^{2+}$, was synthesized by combining $^{i}Pr_3$-tren and $Cu(ClO_4)_2{\cdot}H_2O$ in acetonitrile and characterized using UV-vis, electrospray ionization mass spectrometry (ESI-MS) and X-ray crystallography (see the Supplementary Methods, Supplementary Tables 1 and 2, and Supplementary Figs. 1 and 2). The copper(II)-hydroperoxo complex, $[Cu(^{i}Pr_3\text{-tren})(OOH)]^+$ (**1**), was generated by the addition of 5 equiv of H_2O_2 and 2 equiv of TEA to $[Cu(^{i}Pr_3\text{-tren})(CH_3CN)]^{2+}$ in CH_3OH at −50 °C (Fig. 2). Spectrophotometric titration used to monitor the formation of **1** revealed that 5 equiv of H_2O_2 is required for full formation (Supplementary Fig. 3). The intermediate **1** is observed to be metastable (e.g., ca. 5% decay for 1 h at −50 °C). The color of the solution changed from blue to green, with the final solution showing an intense band at 360 nm ($\varepsilon = 1300\ M^{-1}\ cm^{-1}$) and two weak bands at 656 ($\varepsilon = 230\ M^{-1}\ cm^{-1}$) and 830 nm ($\varepsilon = 270\ M^{-1}\ cm^{-1}$) in the UV-vis spectrum, which are characteristic features of Cu(II)-hydroperoxo complexes (Fig. 3a)[18–24]. The former band has been assigned to a LMCT band of the Cu(II)-OOH species, and the latter bands to the d-d transitions of the Cu(II) ion bearing a trigonal bipyramidal structure.

The CSI-MS spectrum of **1** supported the formation of Cu(II)-hydroperoxo species, $[Cu(^{i}Pr_3\text{-tren})(OOH)]^+$ (**1**-$^{16}O_2H$) at a mass-to-charge ratio (m/z) of 368.2 (calcd m/z 368.2; Fig. 3b, red line), together with some unidentified species presumably resulting from the thermal instability of **1** (Supplementary Fig. 4). When the reactions were carried out with isotopically labeled $H_2{}^{18}O_2$ in CH_3OH and $^2H_2O_2$ in CH_3O^2H, mass peaks corresponding to $[Cu(^{i}Pr_3\text{-tren})(^{18}O^{18}OH)]^+$ (**1**-$^{18}O_2H$) (Fig. 3b, blue line) and $[Cu(^{i}Pr_3\text{-tren})(OO^2H)]^+$ (**1**-$O_2{}^2H$) (Fig. 3b, green line) were observed at m/z 372.2 (calcd m/z 372.2) and 369.2 (calcd m/z 369.2), respectively. The four-mass unit shift upon substitution of ^{16}O with ^{18}O demonstrates that **1** contains two oxygen atoms. The one-mass unit shift in a deuterium isotope experiment verifies the existence of a hydroperoxide ligand in **1**. The rRaman spectrum of **1** was collected using 405 nm excitation in CH_3OH at −30 °C (Fig. 3a, inset). **1**-$^{16}O_2H$ exhibits two isotope sensitive bands at 834 and 501 cm^{-1}, which shifted to 790 and 482 cm^{-1}, respectively, in **1**-$^{18}O_2H$. The results support the assignments of these features as O–O and Cu–O stretching vibration on the basis of $^{16\text{-}18}\Delta$ value of 44 and 19 cm^{-1} ($^{16\text{-}18}\Delta$ (calcd) = 48 and 23 cm^{-1} for diatomic harmonic oscillator), respectively[18–24]. Upon ^2H-substitution in **1**, the characteristic Cu–O and O–O stretching vibrational features exhibited a 2-cm^{-1} downshift each (Supplementary Fig. 5), which is comparable to those of a number of metal-hydroperoxo species (Supplementary Table 3)[24–30].

The EPR spectrum of a frozen solution of **1** at 113 K shows a reverse axial signal with $g_\perp = 2.26$ ($A_\perp = 108$ G) and $g_\parallel = 2.06$ ($A_\parallel = 70$ G), which is typical for trigonal bipyramidal five-coordinate Cu(II) complexes (Fig. 3c; see also Supplementary Fig. 6)[2,18,31–37]. Spin quantification finds that the EPR signal corresponds to 91(6)% of the total copper content in the sample (see Supplementary Methods). All the spectroscopic results clearly show that **1** is assigned to be a Cu(II)-hydroperoxo

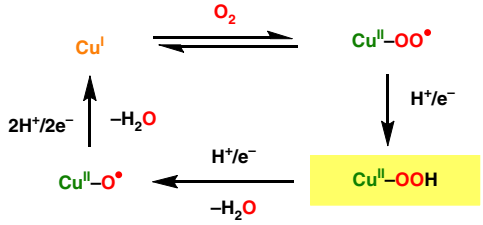

Fig. 1 Bioinorganic context. Representative mechanism of copper intermediates involved in dioxygen activation in metalloenzymes

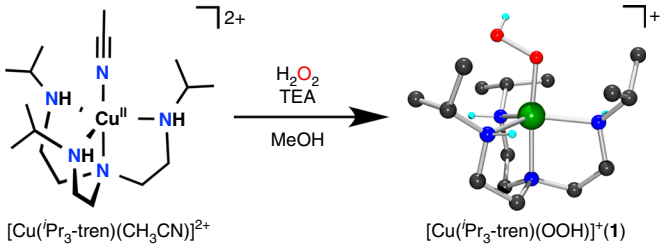

Fig. 2 Synthetic procedure for **1**. DFT structure of **1** (Black, C; Cyan, H; Blue, N; Red, O; Green, Cu). Hydrogen atoms are omitted for clarity except for hydrogen atoms of N–H and O_2–H groups

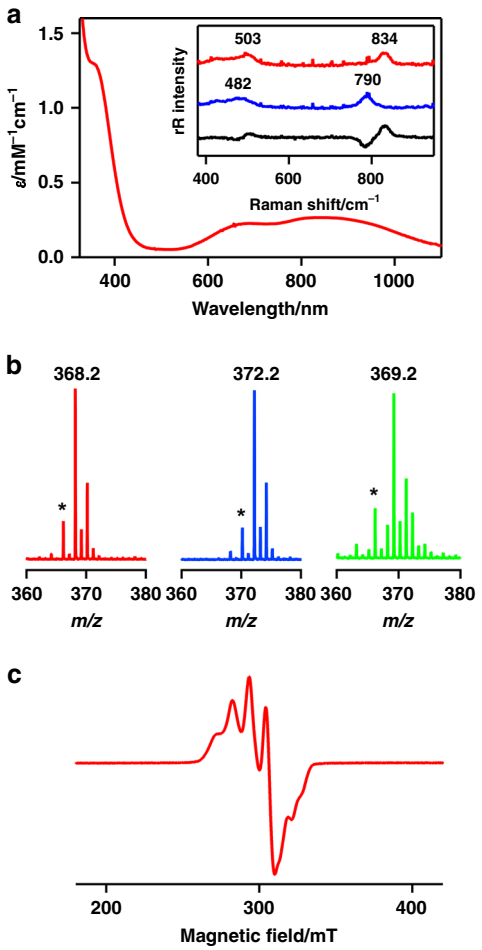

Fig. 3 Characterization of complex **1**. **a** UV-vis spectrum of **1** in CH_3OH at −50 °C. Inset shows the rRaman spectra of **1** (16 mM) prepared with $H_2{}^{16}O_2$ (red line), $H_2{}^{18}O_2$ (blue line), and the difference spectrum (black line), which were obtained upon excitation at 405 nm in CH_3OH at −30 °C. **b** CSI-MS for **1**-$^{16}O_2H$ (red line) and **1**-$^{18}O_2H$ (blue line) in CH_3OH at −40 °C, and for **1**-$O_2{}^2H$ (green line) prepared with $^2H_2O_2$ in CH_3O^2H at −40 °C. Asterisk is assigned to thermally decomposed species of **1**. **c** X-band EPR spectrum of **1** in frozen CH_3OH at 113 K. Spectroscopic settings: frequency = 9.155 GHz, microwave power = 0.998 mW, modulation frequency = 100 kHz, and modulation amplitude = 0.6 mT

complex in trigonal bipyramidal geometry, which is further supported by DFT calculations (vide infra).

Computational study. To investigate the geometric structure of **1**, DFT calculations were conducted at the spin-unrestricted B3LYP level of theory (see Supplementary Methods). The optimized structure of **1** reveals the trigonal bipyramidal geometry whose axial site is occupied by the hydroperoxo group in the manner of end-on replacing an acetonitrile of $[Cu(^iPr_3\text{-tren})(CH_3CN)]^{2+}$ (Fig. 2, and see also Supplementary Table 4). This result is in agreement with the result of EPR spectroscopy described above. The calculated O–O bond distance is determined to be 1.46 Å, which is very close to that determined crystallographically for Masuda's Cu(II)-hydroperoxo complex (1.460 Å)[10] and also that observed for homoprotocatechuate 2,3-dioxygenase (1.5 Å)[38].

TD-DFT calculations were employed to investigate the electronic structure of **1**. The calculated spectrum exhibits an intense peak at 368 nm and multiple weak peaks in the range from 650 to 850 nm which are seen in experimental UV-Vis spectrum (Supplementary Fig. 7). The peak at 368 nm was comprised of electron transitions from overlapped orbitals between the ligand and Cu d-orbitals to σ* orbital of the $d_z{}^2$ orbital in Cu and p_z orbital in O_2H. The minor peaks in the range from 650 to 850 nm are assigned as electron transitions between π* orbitals of Cu-OOH moieties. The singly occupied molecular orbital (SOMO) for **1** was observed to be σ* orbital whose spin density distribution was calculated indicating that about half a radical belongs to Cu center and the rest is contained in the O_2H group and ligand in doublet state (Supplementary Fig. 8; Supplementary Table 5). Natural population analysis (NPA) depicted atomic charges for **1**, which demonstrates that the proximal oxygen atom possesses more negative charge than the distal oxygen atom (Supplementary Fig. 9)[39]. Thus, overall calculations are indicative of a trigonal bipyramidal Cu(II)-hydroperoxo intermediate for **1**.

Reactivity study of 1. The reactivity of **1** was examined in oxidation reaction with organic substrates. The electrophilic reactivity of **1** was tested in the oxidation of triphenylphosphine (i.e., oxygen atom transfer) and cyclohexadiene (i.e., hydrogen atom abstraction). Upon addition of the substrates to **1** in CH_3OH at −50 °C, **1** remained intact without showing any spectral changes (Supplementary Fig. 10). Only trace amounts of products were detected in the product analysis of the reaction solutions. These results indicate that **1** is not capable of oxidizing substrates in electrophilic oxidation under the reaction conditions.

Nucleophilic reaction with acyl chloride. The nucleophilic character of **1** was established in oxidation of acyl chlorides, which are electrophile substrates. On the addition of 100 equiv of benzoyl chloride (PhCOCl) to **1** in CH_3OH at −50 °C, the characteristic absorption bands of **1** disappeared through a first-order decay profile (Fig. 4a). After the reaction was completed, product analysis revealed the formation of benzoic acid in a quantitative yield (Supplementary Table 6). Reaction of **1** with a series of *para*-substituted benzoyl chlorides (*para*-X-PhCOCl, X = OCH_3, CH_3, F, H, Cl) gave a linear correlation of the Hammett plot of the first-order rate constant against $\sigma_p{}^+$ resulting a ρ value of 2.0(3) (Fig. 4b). The positive ρ value indicates nucleophilic character for **1**.

Aldehyde deformylation reaction. It is well known that metal-peroxo species are frequently capable of nucleophilic reactivity. Since it has been reported that the iron-hydroperoxo species is much more reactive than the corresponding iron-peroxo species in aldehyde deformylation[40], the reactivity of **1** was further examined in the oxidation of 2-phenylpropionaldehyde (2-PPA) and cyclohexylcarboxaldehyde (CCA). Kinetic studies of **1** with CCA in CH_3OH at −70 °C exhibit a pseudo-first-order reaction profile (Supplementary Fig. 11). A plot of the first-order rate constants against the concentration of CCA shows a linear correlation, giving a second-order rate constant (k_2) of 6.5(3) M^{-1} s^{-1} (Fig. 5a). Similarly, the k_2 value of $1.5(1)\times10^{-1}$ M^{-1} s^{-1} was determined in the reaction of **1** and 2-PPA at −50 °C (Supplementary Fig. 12b). Cyclohexene (84(9)%) and acetophenone (93 (7)%) were obtained in the oxidation of CCA and 2-PPA, respectively, as final products. Also **1** changed back to the Cu(II) precursor after completion of aldehyde deformylation reaction (Supplementary Fig. 13). The k_2 values were dependent on the reaction temperature where the activation parameters for oxidation of aldehydes by **1** were determined to be $\Delta H^{\ddagger} = 23(1)$ kJ mol^{-1} and $\Delta S^{\ddagger} = -112(2)$ J mol^{-1} K^{-1} in the range of 193–223 K for CCA (Fig. 5b), and $\Delta H^{\ddagger} = 31(1)$ kJ mol^{-1} and $\Delta S^{\ddagger} = -118(7)$ J mol^{-1} K^{-1} in the range of 213–243 K for 2-PPA (Supplementary

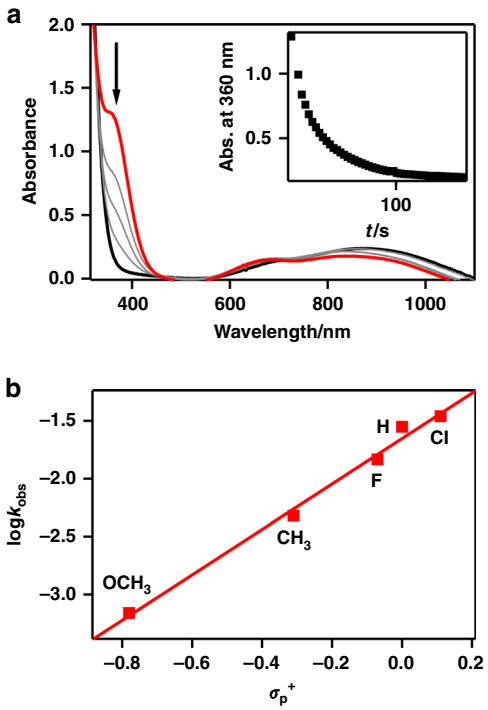

Fig. 4 Reactions of **1** with benzoyl chloride derivatives in CH_3OH at -50 °C. **a** UV-vis spectral changes of **1** (1 mM) upon addition of 100 equiv of benzoyl chloride. Inset shows the time course of the absorbance at 360 nm. **b** Hammett plot of logk_{obs} against σ_p^+ of *para*-X-Ph-COCl (X = OCH_3, CH_3, F, H, Cl)

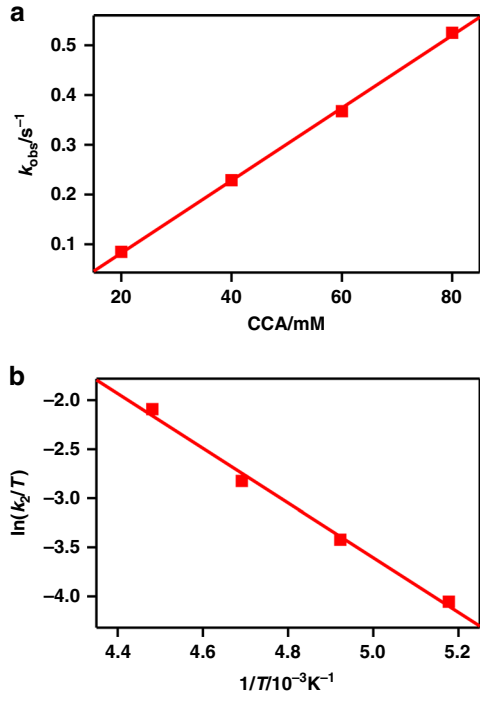

Fig. 5 Reactions of **1** with CCA in CH_3OH. **a** Plot of k_{obs} against CCA concentration to determine a second-order rate constant for **1** at −70 °C. **b** Plot of second-order rate constants against 1/*T* to determine activation parameters

Fig. 12c). A bimolecular mechanism for the nucleophilic oxidative reaction by **1** is suggested by the observed negative entropy and the second-order kinetics. Compared with the reactivity of a previously reported iron(III)-hydroperoxo complex[40] and copper (II)-alkylperoxo adducts[17], the reactivity of **1** ($k_2 = 3.6 \times 10^{-1}$ M^{-1} s^{-1} at −40 °C) is higher than that of the iron(III)-hydroperoxo species ($k_2 = 1.3 \times 10^{-1}$ M^{-1} s^{-1} at −40 °C) and those of copper(II)-alkylperoxo complexes ($k_2 = 1.2–1.8 \times 10^{-1}$ M^{-1} s^{-1} at −40 °C) in aldehyde deformylation of 2-PPA (Supplementary Table 7). It should be noted that the reactivity of **1** ($k_2 =$ 3.4 M^{-1} s^{-1} at −80 °C) with CCA is also higher than that of a Cu(II)-superoxo complex, $[Cu(\beta DK)(O_2)]^-$ ($k_2 = 1.4$ M^{-1} s^{-1} at −80 °C), which was a highly reactive oxidant in aldehyde deformylation reported so far (Supplementary Table 8)[41]. Very recently, it has been reported that an anionic copper(II)-superoxo complex acts as a base than a nucleophile in the aldehyde deformylation of wet 2-PPA[42]. Furthermore, nucleophilic reactivity has been observed for an Fe(III) porphyrin peroxo complex in the epoxidation of electron-deficient olefins[43,44]. Thus, we also explored epoxidation of olefins such as cyclohexene and 2-cyclohexene-1-one, which is an electron-deficient olefin, by **1** in CH_3OH at −50 °C (Supplementary Figs. 14 and 15). Product analyses of the reaction solutions with olefins did not show oxidized products. These results suggest that **1** lacked reactivity in the epoxidation of electron-deficient olefins.

Discussion

Based on the results of kinetic and product analyses, there are two possible initial steps for the nucleophilic reaction, a proximal oxygen attack and a distal oxygen attack by **1** (Fig. 6). The formation of a peroxyhemiacetal intermediate initially proceeds via an attack of the proximal oxygen to the carbonyl center of aldehydes, while the formation of a $[Cu(^iPr_3\text{-tren})]^{2+}$ bound peroxyhemiacetal-like species occurs through a proton transfer and a distal oxygen attack to the aldehydes. The calculated atomic charge distribution of the proximal oxygen (−0.60) from NPA is more negative than that of the distal oxygen (−0.49) (Supplementary Fig. 8), supporting the proximal oxygen attack mechanism. However, the negative charge difference is small. Thus, further detailed DFT studies such as reaction coordinate calculations are under investigation.

In this study, we have demonstrated the oxidation of organic carbonyl compounds by **1**, giving the first, to our knowledge, example of nucleophilic reactivity of a copper(II)-hydroperoxo complex. **1** was characterized by various methods such as UV-vis, CSI-MS, rRaman and EPR. These results clearly indicate that **1** is an end-on Cu(II)-hydroperoxo complex with trigonal bipyramidal coordination geometry, which is also supported by isotope labeling experiments and DFT calculations. The nucleophilic character of **1** was confirmed by a positive slop in the Hammett plot for the reaction of **1** and *para*-substituted acyl chlorides. Kinetic studies represent that **1** is a very reactive nucleophilic

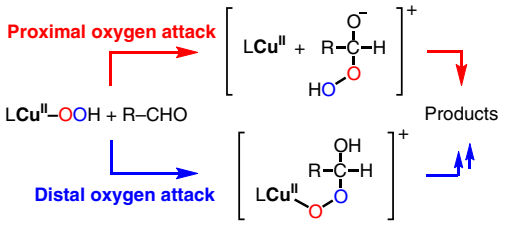

Fig. 6 Proposed mechanism for the reaction of **1** and aldehydes. In both cases the Cu(II)-hydroperoxo complex is proposed to act as a nucleophile

oxidant in aldehyde deformylation. We believe the observed oxidative nucleophilic reactivity of **1** demonstrates a new class of reactivity for Cu(II)-hydroperoxo intermediates.

Methods

Preparation of [Cu(^{i}Pr$_3$-tren)(CH$_3$CN)](ClO$_4$)$_2$. [Cu(^{i}Pr$_3$-tren)(CH$_3$CN)](ClO$_4$)$_2$ was prepared by reacting Cu(ClO$_4$)$_2$·6H$_2$O (0.185 g, 0.50 mmol) and tris[2-(isopropylamino)ethyl]amine (^{i}Pr$_3$-tren) (176.42 μL, 0.50 mmol) in CH$_3$CN (3.0 mL). The mixture was stirred for 12 h, giving a blue solution. Et$_2$O (40 mL) was added to the resulting solution to yield a blue powder, which was collected by filtration, washed with Et$_2$O, and dried in a vacuo. Yield: 97% (0.2799 g). X-ray crystallographically suitable crystals were obtained by slow diffusion of Et$_2$O into a solution of the complex in CH$_3$CN (Supplementary Table 1 and 2; Supplementary Fig. 1). ESI-MS in CH$_3$CN (Supplementary Fig. 2): *m/z* 167.6 for [Cu(^{i}Pr$_3$-tren)]$^{2+}$, *m/z* 188.2 for [Cu(^{i}Pr$_3$-tren)(CH$_3$CN)]$^{2+}$, *m/z* 208.7 for [Cu(^{i}Pr$_3$-tren)(CH$_3$CN)$_2$]$^{2+}$, and *m/z* 434.3 for [Cu(^{i}Pr$_3$-tren)](ClO$_4$)$^+$. Anal. Calcd for C$_{17}$H$_{39}$CuN$_5$O$_8$: C, 35.45; H, 6.82; N, 12.16. Found: C, 35.54; H, 7.05; N, 12.16. The effective magnetic moment of $\mu_{eff} = 1.8$ B.M. was determined by ^{1}H NMR Evans method in CD$_3$CN at 25 °C.

Generation of [Cu(^{i}Pr$_3$-tren)(OOH)]$^+$ (1). Treatment of [Cu(^{i}Pr$_3$-tren)(CH$_3$CN)](ClO$_4$)$_2$ (1 mM) with 5 equiv of H$_2$O$_2$ in the presence of 2 equiv of triethylamine (TEA) in CH$_3$OH at −50 °C afforded a green solution. [Cu(^{i}Pr$_3$-tren)(^{18}O^{18}OH)]$^+$ and [Cu(^{i}Pr$_3$-tren)(OO^{2}H)]$^+$ were prepared by adding 5 equiv of H$_2{}^{18}$O$_2$ (36 μL, 95% ^{18}O-enriched, 2.2% H$_2{}^{18}$O$_2$ in water) and 5 equiv of ^{2}H$_2$O$_2$ (30% in ^{2}H$_2$O), respectively, to a solution containing [Cu(^{i}Pr$_3$-tren)(CH$_3$CN)](ClO$_4$)$_2$ (1 mM) and 2 equiv of TEA in CH$_3$OH at −50 °C. UV-vis in CH$_3$OH: λ_{max} (ε) = 360 nm (1300 M^{-1} cm^{-1}), 656 nm (230 M^{-1} cm^{-1}) and 830 nm (270 M^{-1} cm^{-1}).

X-ray crystallography. See Supplementary Methods, Supplementary Fig. 1, and Supplementary Tables 1 and 2.

Computational details. See Supplementary Methods, Supplementary Figs. 6, 7, and 8, and Supplementary Tables 4 and 5.

Reactivity studies. See Supplementary Methods, Supplementary Figs. 9–14, and Supplementary Tables 6–8.

Data availability

The X-ray crystallographic coordinates for the structures reported in this Article have been deposited at the Cambridge Crystallographic Data Centre (CCDC), under deposition number CCDC-1879280. These data can be obtained free of charge from The Cambridge Crystallographic Data Centre via www.ccdc.cam.ac.uk/ data_request/cif. All other data are available from the corresponding author upon reasonable request.

Received: 22 April 2019 Accepted: 24 June 2019
Published online: 18 July 2019

References

1. Elwell, C. E. et al. Copper−oxygen complexes revisited: structures, spectroscopy, and reactivity. *Chem. Rev.* **117**, 2059–2107 (2017).
2. Solomon, E. I. et al. Copper active sites in biology. *Chem. Rev.* **114**, 3659–3853 (2014).
3. Pettingill, T. M., Strange, R. W. & Blackburn, N. J. Carbonmonoxy dopamine β -hydroxylase. *J. Biol. Chem.* **266**, 16996–17003 (1991).
4. Prigge, S. T., Kolhekar, A. S., Eipper, B. A., Mains, R. E. & Amzel, L. M. Amidation of bioactive peptides: the structure of peptidylglycine α-hydroxylating monooxygenase. *Science* **278**, 1300–1305 (1997).
5. Klinman, J. P. The copper-enzyme family of dopamine β-monooxygenase and peptidylglycine α-hydroxylating monooxygenase: resolving the chemical pathway for substrate hydroxylation. *J. Biol. Chem.* **281**, 3013–3016 (2006).
6. Luisa, C., Gideon, J. D., William, B. T. & Paul, H. W. Bracing copper for the catalytic oxidation of C–H bonds. *Nat. Catal.* **1**, 571–577 (2018).
7. Hemsworth, G. R., Henrissat, B., Davies, G. J. & Walton, P. H. Discovery and characterization of a new family of lytic polysaccharide monooxygenases. *Nat. Chem. Biol.* **10**, 122–126 (2014).
8. Kim, S., Stahlberg, J., Sandgren, M., Paton, R. S. & Beckham, G. T. Quantum mechanical calculations suggest that lytic polysaccharide monooxygenases use a copper-oxyl, oxygen-rebound mechanism. *Proc. Natl Acad. Sci. USA* **111**, 149–154 (2014).
9. Hedegård, E. D. & Ryde, U. Molecular mechanism of lytic polysaccharide monooxygenases. *Chem. Sci.* **9**, 3866–3880 (2018).
10. Wada, A. et al. Structural and spectroscopic characterization of a mononuclear hydroperoxo - copper(II) complex with tripodal pyridylamine ligands. *Angew. Chem. Int. Ed.* **37**, 798–799 (1998).
11. Mann, S. I., Heinisch, T., Ward, T. R. & Borovik, A. S. Peroxide activation Regulated by hydrogen bonds within artificial Cu proteins. *J. Am. Chem. Soc.* **139**, 17289–17292 (2017).
12. Maiti, D., Lucas, H. R., Narducci Sarjeant, A. A. & Karlin, K. D. Aryl hydroxylation from a mononuclear copper-hydroperoxo species. *J. Am. Chem. Soc.* **129**, 6998–6999 (2007).
13. Kim, S. et al. Amine oxidative N-dealkylation via cupric hydroperoxide Cu–OOH homolytic cleavage followed by site-specifc fenton chemistry. *J. Am. Chem. Soc.* **137**, 2867–2874 (2015).
14. Maiti, D., Sarjeant, A. A. N. & Karlin, K. D. Copper-hydroperoxo-mediated N-debenzylation chemistry mimicking aspects of copper monooxygenases. *Inorg. Chem.* **47**, 8736–8747 (2008).
15. Li, L., Sarjeant, A. A. N. & Karlin, K. D. Reactivity study of a hydroperoxodicopper(II) complex: hydroxylation, dehydrogenation, and ligand cross-link reactions. *Inorg. Chem.* **45**, 7160–7172 (2006).
16. Li, L. et al. Exogenous nitrile substrate hydroxylation by a new dicopper-hydroperoxide complex. *J. Am. Chem. Soc.* **127**, 15360–15361 (2005).
17. Kim, B., Jeong, D. & Cho, J. Nucleophilic reactivity of copper(II)–alkylperoxo complexes. *Chem. Commun.* **53**, 9328–9331 (2017).
18. Choi, Y. J. et al. Spectroscopic and computational characterization of Cu^{II}–OOR (R = H or cumyl) complexes bearing a Me$_6$-tren ligand. *Dalton Trans.* **40**, 2234–2241 (2011).
19. Yamaguchi, S. et al. Synthesis, characterization, and thermal stability of new mononuclear hydrogenperoxocopper(II) complexes with N$_3$O-type tripodal ligands bearing hydrogen-bonding interaction sites. *Bull. Chem. Soc. Jpn* **78**, 116–124 (2005).
20. Yamaguchi, S. et al. Thermal stability of mononuclear hydroperoxocopper(II) species. Effects of hydrogen bonding and hydrophobic field. *Chem. Lett.* **33**, 1556–1557 (2004).
21. Fujii, T. et al. Mononuclear copper(II)–hydroperoxo complex derived from reaction of copper(I) complex with dioxygen as a model of Dβ M and PHM. *Chem. Commun.* **0**, 4428–4430 (2006).
22. Yamaguchi, S. et al. Copper hydroperoxo species activated by hydrogen-bonding interaction with its distal oxygen. *Inorg. Chem.* **42**, 6968–6970 (2003).
23. Kim, S., Saracini, C., Siegler, M. A., Drichko, N. & Karlin, K. D. Coordination chemistry and reactivity of a cupric hydroperoxide species featuring a proximal H-bonding substituent. *Inorg. Chem.* **51**, 12603–12605 (2012).
24. Chen, P., Fujisawa, K. & Solomon, E. I. Spectroscopic and theoretical studies of mononuclear copper(II) alkyl- and hydroperoxo complexes: electronic structure contributions to reactivity. *J. Am. Chem. Soc.* **122**, 10177–10193 (2000).
25. Denisov, I. G., Mak, P. J., Makris, T. M., Sligar, S. G. & Kincaid, J. R. Resonance raman characterization of the peroxo and hydroperoxo intermediates in cytochrome P450. *J. Phys. Chem. A* **112**, 13172–13179 (2008).
26. Mak, P. J., Thammawichai, W., Wiedenhoeft, D. & Kincaid, J. R. Resonance Raman spectroscopy reveals pH-dependent active site structural changes of lactoperoxidase compound 0 and its ferryl heme O–O bond cleavage products. *J. Am. Chem. Soc.* **137**, 349–361 (2015).
27. Ibrahim, M., Denisov, I. G., Makris, T. M., Kincaid, J. R. & Sligar, S. G. Resonance raman spectroscopic studies of hydroperoxo-myoglobin at cryogenic temperatures. *J. Am. Chem. Soc.* **125**, 13714–13718 (2003).
28. Mak, P. J. et al. Resonance Raman detection of the hydroperoxo intermediate in the cytochrome P450 enzymatic cycle. *J. Am. Chem. Soc.* **129**, 6382–6383 (2007).
29. He, C. et al. Diiron complexes of 1,8-naphthyridine-based dinucleating ligands as models for hemerythrin. *J. Am. Chem. Soc.* **122**, 12683–12690 (2000).
30. Mak, P. J. & Kincaid, J. R. Resonance Raman spectroscopic studies of hydroperoxo derivatives of cobalt-substituted myoglobin. *J. Inorg. Biochem.* **102**, 1952–1957 (2008).
31. Lucchese, B. et al. Mono-, bi-, and trinuclear Cu^{II}-Cl containing products based on the tris(2-pyridylmethyl)amine chelate derived from copper(I) complex dechlorination reactions of chloroform. *Inorg. Chem.* **43**, 5987–5998 (2004).
32. Barbucci, R., Bencini, A. & Gatteschi, D. Electron spin resonance spectra and spin-hamiltonian parameters for trigonal-bipyramidal nickel(I) and copper(II) complexes. *Inorg. Chem.* **16**, 2117–2120 (1977).
33. Kooter, I. M. et al. EPR characterization of the mononuclear Cu-containing *aspergillus japonicus* quercetin 2,3-dioxygenase reveals dramatic changes upon anaerobic binding of substrates. *Eur. J. Biochem.* **269**, 2971–2979 (2002).
34. Addison, A. W., Hendriks, H. M. J., Reedijk, J. & Thompson, L. K. Copper complexes of the "tripod" ligand tris(2-benzimidazolylmethyl)amine: five- and six-coordinate copper(II) derivatives and some copper(I) derivatives. *Inorg. Chem.* **20**, 103–110 (1981).

35. Thompson, L. K., Ramaswamy, B. S. & Dawe, R. D. Nickel(II) and copper(II) complexes of the 'tripod' ligand tris(2-benzimidazylmethy1)amine. *Can. J. Chem.* **56**, 1311–1318 (1978).
36. Senyukova, G. A., Mikheikin, I. D. & Zamaraev, K. I. EPR spectra of the complex $[Cu(tren)OH]^+$ which has a trigonal bipyramidal structure. *J. Struct. Chem.* **11**, 18–21 (1970).
37. Jiang, F., Karlin, K. D. & Peisach, J. An electron spin echo envelope modulation (ESEEM) study of electron-nuclear hyperfine and nuclear quadrupole interactions of d_z^2 ground state copper(II) complexes with substituted imidazoles. *Inorg. Chem.* **32**, 2576–2582 (1993).
38. Kovaleva, E. G. & Lipscomb, J. D. Crystal structures of Fe^{2+} dioxygenase superoxo, alkylperoxo, and bound product intermediates. *Science* **316**, 453–457 (2007).
39. Panda, C. et al. Nucleophilic versus electrophilic reactivity of bioinspired superoxido nickel(II) complexes. *Angew. Chem. Int. Ed.* **57**, 14883–14887 (2018).
40. Cho, J. et al. Structure and reactivity of a mononuclear non-haem iron(III)-peroxo complex. *Nature* **478**, 502–505 (2011).
41. Pirovano, P. et al. Nucleophilic reactivity of a copper(II)–superoxide complex. *Angew. Chem. Int. Ed.* **53**, 5946–5950 (2014).
42. Bailey, W. D. et al. Revisiting the synthesis and nucleophilic reactivity of an anionic copper-superoxide complex. *Inorg. Chem.* **58**, 4706–4711 (2019).
43. Sisemore, M. F., Burstyn, J. N. & Valentine, J. S. Epoxidation of electron-deficient olefins by a nucleophilic iron(III) peroxo porphyrinato complex, peroxo(tetramesitylporphyrinato)ferrate(1-). *Angew. Chem. Int. Ed. Engl.* **35**, 206–208 (1996).
44. Selke, M. & Valentine, J. S. Switching on the nucleophilic reactivity of a ferric porphyrin peroxo complex. *J. Am. Chem. Soc.* **120**, 2652–2653 (1998).

Acknowledgements

The research was supported by NRF (2017R1A2B4005441 and 2018R1A5A1025511 to J.C.) and the Ministry of Science, ICT and Future Planning (CGRC 2016M3D3A01913243 to J.C.) of Korea, and the Ministry of Education, Culture, Sports, Science and Technology of Japan through the "Strategic Young Researcher Overseas Visits Program for Accelerating Brain Circulation to T.O.". We thank Profs. Sachiko Yanagisawa and Minoru Kubo for assistance in acquiring rRaman spectra.

Author contributions

B.K. and J.C. conceived and designed the experiments; B.K., D.J., and T.O. performed the experiments; B.K., D.J., and J.C. analyzed the data; B.K., D.J., and J.C. co-wrote the paper.

Additional information

Supplementary information accompanies this paper at https://doi.org/10.1038/s42004-019-0187-3.

Competing interests: The authors declare no competing interests.

Reprints and permission information is available online at http://npg.nature.com/reprintsandpermissions/

Publisher's note: Springer Nature remains neutral with regard to jurisdictional claims in published maps and institutional affiliations.